AIAA JOURNAL
Vol. 36, No. 12, December 1998

Optimal Control of Laminated Plate with Piezoelectric Sensor and Actuator Layers

M. C. Ray*
Catholic University of America, Washington, D.C. 20064

A closed-form solution for the optimal control of vibrations of a simply supported symmetric thin laminated plate integrated with piezoelectric layers is obtained. The piezoelectric layers act as the distributed sensors and actuators. The method of designing the optimal steady-state regulator with output feedback is employed. Responses for various design parameters are illustrated. The results may be useful for the purpose of comparing the numerical models and experimental results.

Introduction

APPLICATION of piezoelectric materials as distributed sensors and actuators coupled with elastic structures has attained a great deal of importance for the purpose of active control of structural vibrations.[1–14] The linear quadratic regulators (LQR) with either full state feedback or output feedback are the most effective and widely used modern applied optimal controllers. The LQR with full state feedback has some important guaranteed robustness properties in comparison with the LQR with output feedback.[15] However, in practice, it is difficult to measure all of the states of highly distributed systems like plates and shells. Hence it is apparent that for such systems the linear quadratic control with output feedback may be the feasible means of optimal control.

A literature survey reveals that the papers on optimal control with output feedback using piezoelectric actuators and sensors[10,12] are very few and are concerned with simple beam-type structures. Also, closed-form solutions for such control appear to be lacking in the literature. The objective of this paper is to present a simple method of closed-form solution for optimal control of thin symmetric laminated plates with output feedback using distributed piezoelectric sensors and actuators.

Plant Model

The plate configuration consists of a specially orthotropic laminated plate integrated with piezoelectric layers on its top and bottom surfaces as shown in Fig. 1. The top piezoelectric layer acts as the actuator and the bottom one as the sensor. The overall structure is an N-layered rectangular plate with sides $\boldsymbol{a}$ and $\boldsymbol{b}$. In the present study, the plate is considered as thin and is symmetric about its midplane. Hence, Kirchhoff's plate theory can be adopted to model the plate deformations. Therefore, the in-plane displacements $\boldsymbol{u}$ and $\boldsymbol{v}$ at any point of the plate in the $\boldsymbol{x}$ and $\boldsymbol{y}$ directions, respectively, are given by

$$\boldsymbol{u} = -\boldsymbol{z}\frac{\partial \boldsymbol{w}}{\partial \boldsymbol{x}}, \qquad \boldsymbol{v} = -\boldsymbol{z}\frac{\partial \boldsymbol{w}}{\partial \boldsymbol{y}} \tag{1}$$

where $\boldsymbol{w}$ is the transverse displacement that is constant across the thickness of the plate. The surfaces of the piezolayers that are in contact with the laminated substrate are considered to be suitably grounded. Hence, the electric potential function ϕ^N for the actuator layer that yields zero potential at its interface with the substrate as well as linear variation across its thickness is considered as[16]

$$\phi^N(\boldsymbol{x},\boldsymbol{y},\boldsymbol{z},\boldsymbol{t}) = (\boldsymbol{z} - \boldsymbol{h}_N/\boldsymbol{h}_p)\phi_0^N(\boldsymbol{x},\boldsymbol{y},\boldsymbol{t}), \qquad \boldsymbol{h}_{N+1} \geq \boldsymbol{z} \geq \boldsymbol{h}_N \tag{2}$$

where ϕ^N is the generalized electric potential coordinate and $\boldsymbol{h}_p$ is the thickness of the actuator layer.

The quasistatic constitutive equations for the piezoelectric material are[17]

$$\begin{aligned} \{\boldsymbol{D}^k\} &= [\boldsymbol{e}]^T\{\epsilon^k\} + [\varepsilon]\{\boldsymbol{E}^k\} \qquad (\boldsymbol{k} = 1 \text{ and } \boldsymbol{N}) \\ \{\sigma^k\} &= [\boldsymbol{C}^k]\{\epsilon^k\} - [\boldsymbol{e}]\{\boldsymbol{E}^k\} \qquad (\boldsymbol{k} = 1 \text{ and } \boldsymbol{N}) \end{aligned} \tag{3}$$

and the constitutive equation for the orthotropic material of the substrate is[18]

$$\{\sigma^k\} = [\boldsymbol{C}^k]\{\epsilon^k\} \qquad (\boldsymbol{k} = 2, 3, \ldots, \boldsymbol{N}-1) \tag{4}$$

where $\{\boldsymbol{D}^k\}$, $\{\boldsymbol{E}^k\}$, $\{\sigma^k\}$, and $\{\epsilon^k\}$ represent the vectors of electric displacement, electric field, stress, and strain, respectively; and $[\boldsymbol{e}^k]$, $[\epsilon^k]$, and $[\boldsymbol{C}^k]$ denote the matrices of piezoelectric constants, dielectric constants, and elastic constants, respectively.

The electric field potential relation is given by

$$\boldsymbol{E}^k_{x_i} = -\frac{\partial \phi^k}{\partial \boldsymbol{x}_i} \qquad (\boldsymbol{x}_i = \boldsymbol{x}, \boldsymbol{y}, \boldsymbol{z}, \boldsymbol{k} = 1 \text{ and } \boldsymbol{N}) \tag{5}$$

The potential energy of the overall plate can be written as[17]

$$\begin{aligned} \boldsymbol{T}_p = {} & \frac{1}{2}\sum_{k=1}^{N}\int_{h_k}^{h_{k+1}}\int_0^b\int_0^a \{\epsilon^k\}^T\{\sigma^k\}\,\mathrm{d}\boldsymbol{x}\,\mathrm{d}\boldsymbol{y}\,\mathrm{d}\boldsymbol{z} \\ & - \frac{1}{2}\sum_{k=1}^{N}\int_{h_k}^{h_{k+1}}\int_0^b\int_0^a \{\boldsymbol{E}^N\}^T\{\boldsymbol{D}^N\}\,\mathrm{d}\boldsymbol{x}\,\mathrm{d}\boldsymbol{y}\,\mathrm{d}\boldsymbol{z} \\ & - \int_0^b\int_0^a \boldsymbol{p}(\boldsymbol{x},\boldsymbol{y},\boldsymbol{t})\Big|_{z=h_{N+1}} \boldsymbol{w}\,\mathrm{d}\boldsymbol{x}\,\mathrm{d}\boldsymbol{y} \\ & + \int_0^b\int_0^a \bar{\sigma}(\boldsymbol{x},\boldsymbol{y},\boldsymbol{t})\Big|_{z=h_{N+1}} \mathrm{d}\boldsymbol{x}\,\mathrm{d}\boldsymbol{y} \end{aligned} \tag{6}$$

and the total kinetic energy of the plate is

$$\boldsymbol{T}_K = \frac{1}{2}\sum_{k=1}^{N}\int_{h_k}^{h_{k+1}}\int_0^b\int_0^a \rho^k(\dot{\boldsymbol{u}}^2 + \dot{\boldsymbol{v}}^2 + \dot{\boldsymbol{w}}^2)\,\mathrm{d}\boldsymbol{x}\,\mathrm{d}\boldsymbol{y}\,\mathrm{d}\boldsymbol{z} \tag{7}$$

where $\boldsymbol{p}(\boldsymbol{x},\boldsymbol{y},\boldsymbol{t})$ is the applied transverse load, $\bar{\sigma}(\boldsymbol{x},\boldsymbol{y},\boldsymbol{t})$ is the externally applied surface charge density, and ρ^k is the density of the $\boldsymbol{k}$th layer. Because there is no applied electric field in the sensor, the converse effect of the weak electric field induced by the developed charge in the sensor layer due to its deformation is neglected to evaluate the total potential energy of the plate.

Received Jan. 18, 1997; revision received July 21, 1998; accepted for publication July 24, 1998.

*Postdoctoral Fellow, Mechanical Engineering Department; currently Assistant Professor, Mechanical Engineering Department, Indian Institute of Technology, Guwahati 781 001, India.

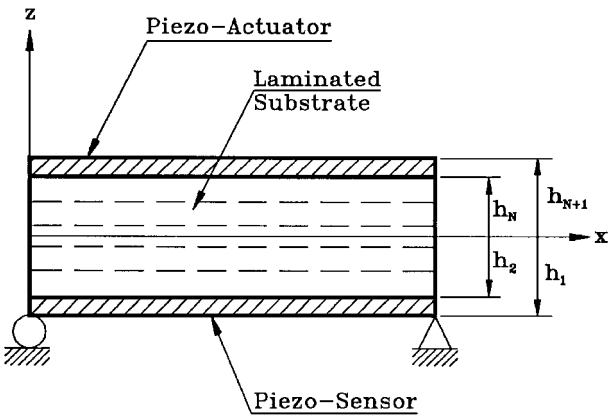

Fig. 1 Plate configuration.

The piezoelectric material considered here is biaxially polarized polyvinylidene fluoride (PVDF), for which the matrices $[e]$ and $[\varepsilon]$ are given by[4]

$$[e]^T = \begin{bmatrix} 0 & 0 & 0 & 0 & 0 & 0 \\ 0 & 0 & 0 & 0 & 0 & 0 \\ e_{31} & e_{31} & 0 & 0 & 0 & 0 \end{bmatrix}$$

and (8)

$$[\varepsilon] = \begin{bmatrix} \varepsilon_{11} & 0 & 0 \\ 0 & \varepsilon_{22} & 0 \\ 0 & 0 & \varepsilon_{33} \end{bmatrix}$$

Using Eqs. (1–5) and Eq. (8) and carrying out the explicit integration with respect to z, one can express Eqs. (6) and (7) as

$$T_p = \int_0^b \int_0^a \left\{ \frac{1}{2} D_{11} \left(\frac{\partial^2 w}{\partial x^2} \right)^2 + D_{12} \frac{\partial^2 w}{\partial x^2} \frac{\partial^2 w}{\partial y^2} + \frac{1}{2} D_{22} \left(\frac{\partial^2 w}{\partial y^2} \right)^2 + 2 D_{66} \left(\frac{\partial^2 w}{\partial x \partial y} \right)^2 - \frac{1}{2} e_{31} (h_{N+1} + h_N) \phi_0^N \left(\frac{\partial^2 w}{\partial x^2} + \frac{\partial^2 w}{\partial y^2} \right) - \frac{1}{6} h_p \left[\varepsilon_{11} \left(\frac{\partial \phi_0^N}{\partial x} \right)^2 + \varepsilon_{22} \left(\frac{\partial \phi_0^N}{\partial y} \right)^2 \right] - \frac{\varepsilon_{33}}{h_p} \left(\phi_0^N \right)^2 - p w + \bar{\sigma} \phi_0^N \right\} dx\, dy \tag{9}$$

and

$$T_K = \frac{1}{2} \int_0^b \int_0^a \left[\bar{m} \dot{w}^2 + I \left(\frac{\partial \dot{w}}{\partial x} \right)^2 + I \left(\frac{\partial \dot{w}}{\partial y} \right)^2 \right] dx\, dy \tag{10}$$

where

$$D_{ij} = \sum_{k=1}^{N} C_{ij} \left(h_{k+1}^3 - h_k^3 \right), \qquad \bar{m} = \sum_{k=1}^{N} \rho^k (h_{k+1} - h_k)$$

$$I = \sum_{k=1}^{N} \frac{1}{3} \rho^k \left(h_{k+1}^3 - h_k^3 \right)$$

Applying Hamilton's variational principle,[17]

$$\delta \int_{t_1}^{t_2} (T_k - T_p)\, dt = 0 \tag{11}$$

and the following governing coupled electromechanical equations are obtained:

$$D_{11} \frac{\partial^4 w}{\partial x^4} + 2(D_{12} + 2D_{66}) \frac{\partial^4 w}{\partial x^2 \partial y^2} + D_{22} \frac{\partial^4 w}{\partial y^4} - \frac{1}{2} e_{31} (h_{N+1} + h_N) \times \left(\frac{\partial^2 \phi_0^N}{\partial x^2} + \frac{\partial^2 \phi_0^N}{\partial y^2} \right) + \bar{m} \ddot{w} - I \frac{\partial^2 \ddot{w}}{\partial x^2} - I \frac{\partial^2 \ddot{w}}{\partial y^2} = p \tag{12}$$

$$\frac{1}{2} e_{31} (h_{N+1} + h_N) \left(\frac{\partial^2 w}{\partial x^2} + \frac{\partial^2 w}{\partial y^2} \right) - \frac{1}{3} h_p \left(\varepsilon_{11} \frac{\partial^2 \phi_0^N}{\partial x^2} + \varepsilon_{22} \frac{\partial^2 \phi_0^N}{\partial y^2} \right) + \frac{\varepsilon_{33}}{h_p} \phi_0^N = \bar{\sigma} \tag{13}$$

Also, the variational principle yields the following simply supported boundary conditions:

1) Essential boundary conditions

$$w = \phi = 0 \qquad \text{at} \quad x = 0, a \quad \text{and} \quad \text{at} \quad y = 0, b$$

2) Natural boundary conditions

$$D_{11} \frac{\partial^2 w}{\partial x^2} + D_{12} \frac{\partial^2 w}{\partial y^2} - \frac{1}{2} e_{31} (h_{N+1} + h_N) \phi_0^N = 0 \quad \text{at } x = 0 \text{ and } a$$

$$D_{12} \frac{\partial^2 w}{\partial x^2} + D_{22} \frac{\partial^2 w}{\partial y^2} - \frac{1}{2} e_{31} (h_{N+1} + h_N) \phi_0^N = 0 \quad \text{at } y = 0 \text{ and } b \tag{14}$$

Because the piezoelectric layers are fully electroplated on their exposed surfaces, each of them can be treated as a parallel plate capacitor. Thus the uniform voltage V due to the surface charge density $\bar{\sigma}$ across the electrodes of the layer acting as actuator can be given by

$$V = \bar{\sigma} ab / C_p \tag{15}$$

where C_p is the capacitance of this layer. Note that in the closed-loop control system this charge is due to the amplified output of the sensor.

To obtain the closed-form solutions, one expands the unknown variables representing the transverse displacement and the generalized electric potential coordinate into the following double Fourier series representations:

$$w(x, y, t) = \sum_m \sum_n W_{mn}(t) \sin \frac{m\pi x}{a} \sin \frac{n\pi y}{b}$$

$$\phi_0^N(x, y, t) = \sum_m \sum_n \Phi_{mn}(t) \sin \frac{m\pi x}{a} \sin \frac{n\pi y}{b} \tag{16}$$

where $W_{mn}(t)$ and $\Phi_{mn}(t)$ are the time-dependent coefficients to be determined. It is evident that the preceding expressions satisfy the boundary conditions given by Eq. (14). Accordingly, the load function and the applied uniform voltage are also expressed in the same manner as

$$p(x, y, t) = \sum_m \sum_n Q_{mn}(t) \sin \frac{m\pi x}{a} \sin \frac{n\pi y}{b}$$

$$V(x, y, t) = \sum_m \sum_n V_{mn}(t) \sin \frac{m\pi x}{a} \sin \frac{n\pi y}{b} \tag{17}$$

where $Q_{mn}(t)$ and $V_{mn}(t)$ are the time-dependent modal amplitudes of the applied load and voltage, respectively.

Substituting Eqs. (15–17) into Eqs. (12) and (13) and then eliminating $\Phi_{mn}(t)$ from the resulting equations, one obtains the following equation describing the flexural motion of the plate under combined action of mechanical and electrical loading:

$$\ddot{W}_{mn}(t) + \omega_{mn}^2 W_{mn}(t) = \frac{Q_{mn}(t)}{M} - K_c V_{mn}(t) \tag{18}$$

where

$$\omega_{mn}^2 = \frac{1}{M} \left[D_{11} \left(\frac{m\pi}{a} \right)^4 + 2(D_{12} + 2D_{66}) \frac{m^2 n^2 \pi^4}{a^2 b^2} + D_{22} \left(\frac{n\pi}{b} \right)^4 + D_p \right]$$

$$M = \bar{m} + I \left(\frac{m^2 \pi^2}{a^2} + \frac{n^2 \pi^2}{b^2} \right)$$

$$K_c = \frac{3e_{31}(h_{N+1}+h_N)h_p[(m^2\pi^2/a^2)+(n^2\pi^2/b^2)]C_p}{2abM\left\{h_p^2\left[\varepsilon_{11}(m^2\pi^2/a^2)+\varepsilon_{22}(n^2\pi^2/b^2)\right]+3\varepsilon_{33}\right\}}$$

$$D_p = \frac{e_{31}(h_{N+1}+h_N)[(m^2\pi^2/a^2)+(n^2\pi^2/b^2)]MabK_c}{2C_p}$$

Sensor Output

Because of the direct piezoelectric effect, the charge generated in the sensor layer due to its deformation along with the substrate can be collected at the unearthed exposed electroplated surface of the sensor. According to the Gauss law, this charge $q(t)$ is equal to the spatial integration of the electric displacement in the z direction over this electroplated surface as follows[19]:

$$q(t) = \int_0^b \int_0^a D_z\Big|_{z=h_1} \mathrm{d}x\,\mathrm{d}y \tag{19a}$$

Using Eqs. (1), (3), and (16) in Eq. (19a), one can express the output of the sensor as

$$q(t) = \sum_m \sum_n q_{mn}(t) = \sum_m \sum_n F_{mn} W_{mn}(t) \tag{19b}$$

where

$$F_{mn} = \frac{abh_1 e_{31}}{mn\pi^2}\left(\frac{m^2}{a^2}+\frac{n^2}{b^2}\right)[1-(-1)^m][1-(-1)^n]$$

So that this induced charge can be used in the feedback control system, the sensor is augmented with a current amplifier to produce the closed-circuit modal current. Such current measured across the electrodes of the sensor can be determined as[6]

$$i_{mn}(t) = \frac{\mathrm{d}q_{mn}(t)}{\mathrm{d}t} = F_{mn}\dot{W}_{mn}(t) \tag{20}$$

Optimal Control with Output Feedback

In the absence of an applied mechanical load, Eq. (18) can be cast into standard state-space form as

$$\frac{\mathrm{d}X}{\mathrm{d}t} = AX + BV_{mn}(t) \tag{21}$$

where

$$X = [W_{mn}(t) \quad \dot{W}_{mn}(t)/\omega_{mn}]^T, \qquad A = \begin{bmatrix} 0 & \omega_{mn} \\ -\omega_{mn} & 0 \end{bmatrix}$$

and

$$B = [0 \quad -K_c/\omega_{mn}]^T$$

In the closed-loop model, the current output from the sensor as given by Eq. (20) is negatively fed back to the actuator. This results in a generation of surface charge on the electroded surface of the actuator, which after uniform distribution gives rise to a uniform control voltage across the electrodes. Thus, in the closed-loop system, the amplitude of the modal control voltage input to the actuator can be expressed as

$$V_{mn}(t) = -Ki_{mn}(t) = -KC_0X \tag{22}$$

where K is the optimal gain to be determined and $C_0 = [0 \;\; F_{mn}\omega_{mn}]$.

It may be noted from Eq. (22) that the feedback of the output of the sensor generates the control law with reduced state information as manifested by the output matrix C_0. Hence, the optimal control problem turns out to be an LQR problem with output feedback. The optimal regulation of the state may be attained by selecting the control input $V_{mn}(t)$ to minimize a quadratic performance index[15]:

$$J = \int_0^\infty \left\{X^TQX + V_{mn}(t)^TRV_{mn}(t)\right\}\mathrm{d}t \tag{23}$$

where J is the cost function, with Q and R being the positive semidefinite state weighting matrix and positive definite control weighting matrix, respectively. If the closed-loop plant is asymptotically stable, then it is well known that the minimization of the performance index given by Eq. (23) to find the optimal output feedback gain leads to minimizing the cost of the form[15]

$$J = \tfrac{1}{2}\mathrm{tr}\{PX(0)X(0)^T\}, \qquad P \geq 0 \tag{24}$$

in which P is an unknown symmetric positive semidefinite matrix. To relieve Eq. (24) of its dependence on the initial state vector $X(0)$, it is usual that the problem statement is modified slightly to that of minimizing the expected value of J, i.e., $E\{J\}$ (Ref. 20). Then Eq. (24) is to be replaced by

$$E\{J\} = \tfrac{1}{2}\mathrm{tr}(PY) \tag{25}$$

where $Y = E\{X(0)X(0)^T\}$ is the autocorrelation of the initial state vector. In general, the initial states are assumed to be uniformly distributed on the unit sphere such that Y is an identity matrix.[20]

The minimizing process yields the following design equations[15]:

$$A_c^TP + PA_c + C_0^TK^TRKC_0 + Q = 0 \tag{26}$$

$$SA_c^T + A_cS + Y = 0 \tag{27}$$

$$K = R^{-1}B^TPSC_0^T\left(C_0SC_0^T\right)^{-1} \tag{28}$$

wherein $A_c = A - BKC_0$. The unknown matrices P and S are solved from Eqs. (26) and (27), and the optimal value of K is obtained from Eq. (28).

The following algorithm[21] is employed for iterative solutions of Eqs. (26) and (27):

1) Choose an initial value of K such that A_c is stable. Set $i = 0$.

2) Solve Eqs. (26) and (27) for P_i and S_i.

3) Evaluate $\Delta K_i = R^{-1}B^TP_iS_iC_0^T(C_0SC_0^T)^{-1} - K_i$.

4) Set $K_{i+1} = K_i + \alpha\Delta K_i$, where α is chosen at each iteration such that $J_{i+1} < J_i$.

5) Set $i = i + 1$, go to step 2, and repeat the process until convergence is achieved.

An important aspect is to choose the initial value of K. It can be analytically shown that, if the initial value of K is chosen as $-\omega_{mn}/(K_cF_{mn})$, then the closed-loop system will be asymptotically stable.

Results

Using Eq. (22), Eq. (18) is solved. Finally, using Eq. (16), the closed-form solution of the transverse displacement at any point of the plate can be shown to be of the form

$$w(x,y,t) = \sum_m \sum_n e^{\alpha_{mn}t}\left(\cos\beta_{mn}t - \frac{\alpha_{mn}}{\beta_{mn}}\sin\beta_{mn}t\right) \times W_{mn}(0)\sin\frac{m\pi x}{a}\sin\frac{n\pi y}{b} \tag{29}$$

where, for a combination of m and n, the real and imaginary parts α_{mn} and β_{mn}, respectively, of the optimal closed-loop poles are given by

$$\alpha_{mn} = \tfrac{1}{2}KK_cF_{mn}, \qquad \beta_{mn} = \tfrac{1}{2}\sqrt{4\omega_{mn}^2 - K^2K_c^2F_{mn}^2}$$

and $W_{mn}(0)$ is the initial center deflection.

Numerical results are sought for a (0 deg/90 deg/0 deg) square laminate. Each ply of the laminate is made of graphite/epoxy composite for which the following material properties[18] are used: $E_L = 172.5$ GPa, $E_T = E_L/25$, $G_{LT} = 0.5E_T$, $G_{TT} = 0.2E_T$, $\nu_{LT} = \nu_{TT} = 0.25$, and $\rho = 1600$ kg/m^2, where E_L and E_T are Young's moduli; G_{LT} and G_{TT} are the shear moduli; and ν_{LT} and ν_{TT} are major and minor Poisson's ratios, with L and T designating the longitudinal and transverse principle material directions, respectively. The material properties of PVDF are adopted as $E = 2\times10^9$ Pa, $e_{31} = 0.046$ C/m^2, $\varepsilon_{11} = \varepsilon_{22} = \varepsilon_{33} = 1.062\times10^{-10}$ F/m, $C_p = 3.8\times10^{-6}$ F, and $\rho = 1800$ kg/m^3 (Refs. 4 and 13).

The thickness of each ply of the substrate is taken as 1 mm, and that of each piezoelectric layer is 0.5 mm. The length-to-thickness ratio of the plate is 50. The control weighting matrix R is considered as rI, with r being the design parameter. The state weighting

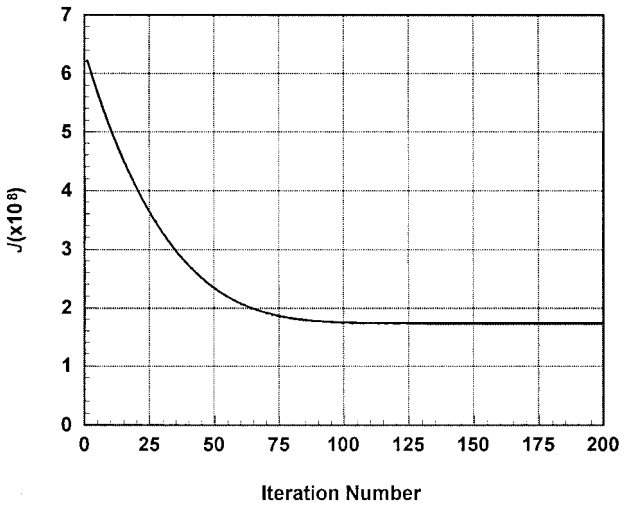

Fig. 2 Convergence of cost function for m and $n = 1$.

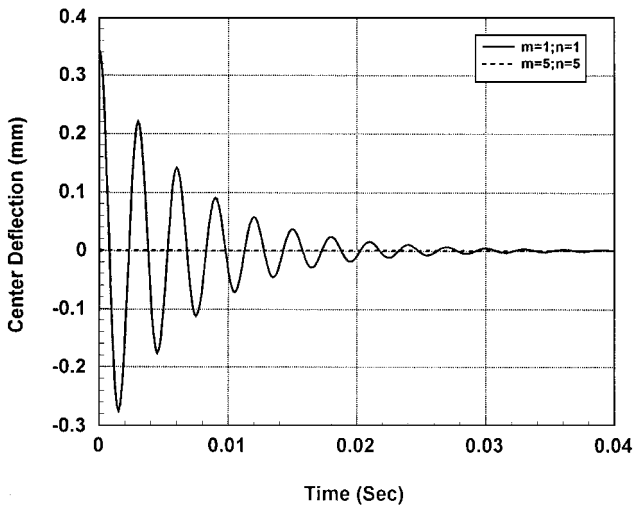

Fig. 3 Convergence of response for m and $n = 5$.

matrix $\boldsymbol{Q}$ is considered as $\boldsymbol{q}\omega_{mn}^2 \boldsymbol{C}_0^T \boldsymbol{C}_0/(\boldsymbol{K}_c^2 \boldsymbol{F}_1^2)$, with $\boldsymbol{q}$ being the design parameter. Figure 2 shows a typical curve obtained by this algorithm to demonstrate that the cost function converges to a minimum value after a certain number of iterations, yielding the optimal gain for $\boldsymbol{m}$ and $\boldsymbol{n} = 1$. A concentrated load of 100 N is applied statically at the center of the plate and then withdrawn to set the plate into transient vibration with initial center deflection. The number of modes required to obtain the converged response is of particular concern. To test the convergence of the solution, the contribution of the higher modes into the controlled response is investigated, as shown in Fig. 3. This figure clearly displays that the contribution of the mode corresponding to $\boldsymbol{m}$ and $\boldsymbol{n} = 5$ is negligible compared with that of the first mode. Also, the sensor equation permits one to consider the modes corresponding to odd $\boldsymbol{m}$ and $\boldsymbol{n}$ only. Thus, the final response is obtained considering a 15-term approximation of the double Fourier series representations of the deflection, control voltage, and sensor output. Figures 4 and 5 illustrate the control of center deflection. The role of design parameters $\boldsymbol{q}$ and $\boldsymbol{r}$ is obvious. For a fixed value of $\boldsymbol{r}$ as the value of $\boldsymbol{q}$ increases, the weighting on the state and, hence, the control force increase and the settling time decreases (Fig. 4). On the other hand, for a particular value of $\boldsymbol{q}$ as the value of $\boldsymbol{r}$ increases, the regulator takes a longer time to derive the state to zero, as shown in Fig. 5. It may be noted from Figs. 4 and 5 that the damping factor increases from 0.072 to 0.168 due to the variation of design parameters. Figure 6 demonstrates the control voltage required for the case cited for Fig. 4. Note that the final response involves finding the optimal gain and closed-loop poles for each combination of $(\boldsymbol{m}, \boldsymbol{n})$ and is presented in Table 1 for different values of $\boldsymbol{m}$ and $\boldsymbol{n}$.

Table 1 Optimal gain and poles ($q = 0.01$ and $r = 0.5$)

m, n	Gain	Poles
1, 1	1.5015×10^5	$-0.1486 \times 10^3 \pm 2.095 \times 10^3$
3, 3	1.5061×10^5	$-0.1334 \times 10^3 \pm 1.8804 \times 10^4$
5, 5	1.5153×10^5	$-3.6861 \times 10^3 \pm 5.1952 \times 10^5$

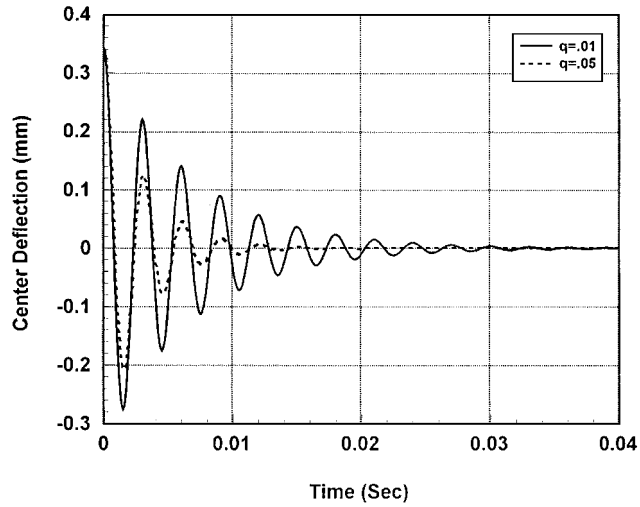

Fig. 4 Center deflection for different values of q and $r = 0.5$.

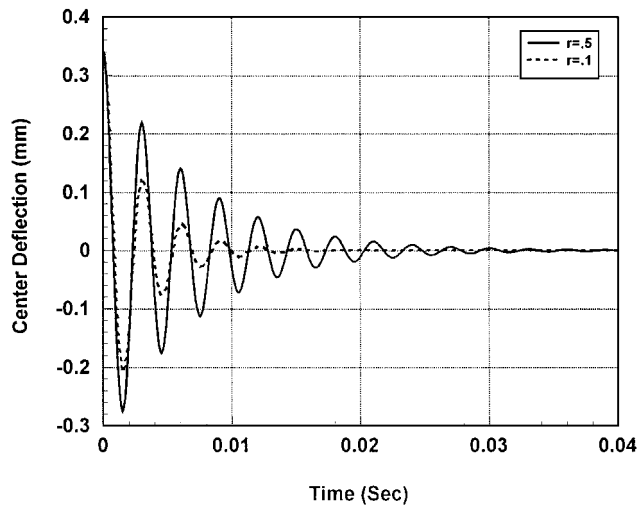

Fig. 5 Center deflection for different values of r and $q = 0.01$.

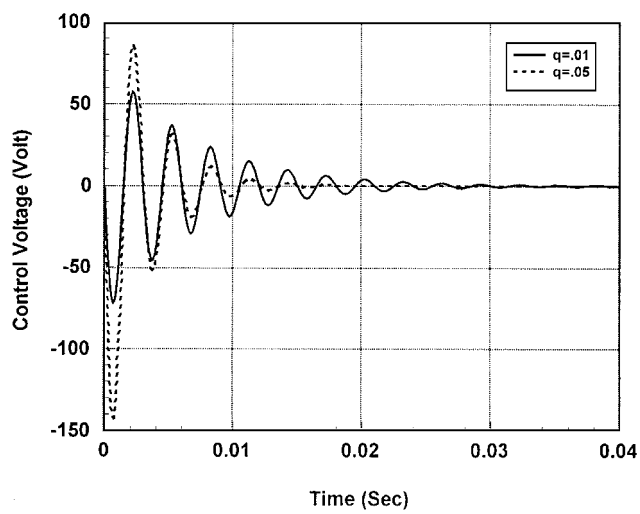

Fig. 6 Control voltage for different values of q and $r = 0.5$.

Conclusion

Optimal control of flexural vibration of a square, simply supported, symmetric, thin laminated plate coupled with piezoelectric sensor and actuator layers is presented. The closed-form solutions of equations of motion of the plate are used to obtain the optimal control solutions. The optimal gain is selected using the method of designing the linear quadratic regulator with output feedback. The contribution of higher modes to the total response is not found to be remarkable. The results may be useful for the purpose of comparing the numerical results. The procedure outlined here can be easily extended to the optimal control of simply supported shells.

References

[1]Bailey, T., and Hubbard, J. E., "Distributed Piezoelectric Polymer Active Vibration Control of a Cantilever Beam," *Journal of Guidance, Control, and Dynamics*, Vol. 8, No. 5, 1985, pp. 605–611.

[2]Crawley, E. F., and Luis, J. D., "Use of Piezoelectric Actuators as Elements of Intelligent Structures," *AIAA Journal*, Vol. 25, No. 10, 1987, pp. 1373–1385.

[3]Baz, A., and Poh, S., "Performance of an Active Control System with Piezoelectric Actuators," *Journal of Sound and Vibration*, Vol. 126, No. 2, 1988, pp. 327–343.

[4]Tzou, H. S., and Tseng, C. I., "Distributed Piezoelectric Sensor/Actuator Design for Dynamic Measurement/Control of Distributed Parameter Systems: A Piezoelectric Finite Element Approach," *Journal of Sound and Vibration*, Vol. 138, No. 1, 1990, pp. 17–34.

[5]Lee, C. K., and Moon, F. C., "Laminated Piezopolymer Plates for Torsion and Bending Sensors and Actuators," *Journal of the Accoustical Society of America*, Vol. 85, No. 6, 1989, pp. 2432–2439.

[6]Lee, C. K., Chiang, W. W., and Sullivan, O., "Piezoelectric Modal Sensor/Actuator Pairs for Critical Active Damping Vibration Control," *Journal of the Accoustical Society of America*, Vol. 90, No. 1, 1991, pp. 374–384.

[7]Hanagud, S., Obal, M. W., and Calise, A. J., "Optimal Vibration Control by the Use of Piezoceramic Sensors and Actuators," *Journal of Guidance, Control, and Dynamics*, Vol. 15, No. 5, 1992, pp. 1199–1206.

[8]Chandrashekara, K., and Agarwal, A. N., "Active Vibration Control of Laminated Composite Plates Using Piezoelectric Devices: A Finite Element Approach," *Journal of Intelligent Material Systems and Structures*, Vol. 4, No. 4, 1993, pp. 496–508.

[9]Samanta, B., Ray, M. C., and Bhattacharyya, R., "Finite Element Model for Active Control of Intelligent Structures," *AIAA Journal*, Vol. 34, No. 9, 1996, pp. 1885–1893.

[10]Baz, A., and Poh, S., "Optimal Vibration Control with Modal Positive Position Feedback," *Optimal Control Applications and Methods*, Vol. 17, 1996, pp. 141–149.

[11]Kang, Y. K., Park, H. C., Hwang, W. W., and Han, K. S., "Optimum Placement of Piezoelectric Sensor/Actuator for Vibration Control of Laminated Beams," *AIAA Journal*, Vol. 34, No. 9, 1996, pp. 1921–1926.

[12]Yang, S. M., and Lee, Y. J., "Optimization of Non-Collocated Sensor/Actuator Location and Feedback Gain in Control Systems," *Smart Materials and Structures*, Vol. 2, No. 2, 1993, pp. 96–102.

[13]Sunar, M., and Rao, S. S., "Distributed Modelling and Actuator Location for Piezoelectric Control Systems," *AIAA Journal*, Vol. 34, No. 10, 1996, pp. 2209–2211.

[14]Birman, V., and Adali, S., "Vibration Damping Using Piezoelectric Stiffener-Actuators with Application to Orthotropic Plates," *Composite Structures*, Vol. 35, 1996, pp. 251–261.

[15]Lewis, F. L., *Applied Optimal Control and Estimation*, Prentice–Hall, Englewood Cliffs, NJ, 1992, Chap. 4.

[16]Ray, M. C., Bhattacharyya, R., and Samanta, S., "Exact Solutions for Static Analysis of Intelligent Structures," *AIAA Journal*, Vol. 31, No. 9, 1993, pp. 1684–1691.

[17]Tiersten, H. F., *Linear Piezoelectric Plate Vibration*, Plenum, New York, 1969, Chap. 6.

[18]Pagano, N. J., "Exact Solutions for Rectangular Bidirectional Composites and Sandwich Plates," *Journal of Composite Material*, Vol. 4, 1970, pp. 20–34.

[19]Griffiths, D. J., *Introduction to Electrodynamics*, Prentice–Hall of India, New Delhi, India, 1991, Chap. 4.

[20]Levine, W. S., and Athans, M., "On the Determination of the Optimal Constant Output Feedback Gains for Linear Multivariable Systems," *IEEE Transactions on Automatic Control*, Vol. AC-15, 1970, pp. 44–48.

[21]Moerder, D. D., and Calise, A. J., "Convergence of a Numerical Algorithm for Calculating Optimal Output Feedback Gains," *IEEE Transactions on Automatic Control*, Vol. AC-30, 1985, pp. 900–903.

R. K. Kapania
Associate Editor